

Akzeptierter Artikel

Titel: Design of Metal-Free Polymer Carbon Dots: a New Class of Room-Temperature Phosphorescent Materials

Autoren: Songyuan Tao, Siyu Lu, Yijia Geng, Shoujun Zhu, Simon Redfern, Yubin Song, Tanglue Feng, Weiqing Xu, and Bai Yang

Dieser Beitrag wurde nach Begutachtung und Überarbeitung sofort als "akzeptierter Artikel" (Accepted Article; AA) publiziert und kann unter Angabe der unten stehenden Digitalobjekt-Identifizierungsnummer (DOI) zitiert werden. Die deutsche Übersetzung wird gemeinsam mit der endgültigen englischen Fassung erscheinen. Die endgültige englische Fassung (Version of Record) wird ehestmöglich nach dem Redigieren und einem Korrekturgang als Early-View-Beitrag erscheinen und kann sich naturgemäß von der AA-Fassung unterscheiden. Leser sollten daher die endgültige Fassung, sobald sie veröffentlicht ist, verwenden. Für die AA-Fassung trägt der Autor die alleinige Verantwortung.

Zitierweise: *Angew. Chem. Int. Ed.* 10.1002/anie.201712662
Angew. Chem. 10.1002/ange.201712662

Link zur VoR: <http://dx.doi.org/10.1002/anie.201712662>
<http://dx.doi.org/10.1002/ange.201712662>

Design of Metal-Free Polymer Carbon Dots: a New Class of Room-Temperature Phosphorescent Materials

Songyuan Tao⁺, Siyu Lu⁺, Yijia Geng, Shoujun Zhu, Simon A. T Redfern, Yubin Song, Tanglue Feng, Weiqing Xu and Bai Yang*

Abstract: Polymer carbon dots (PCDs) are proposed as a new class of room temperature phosphorescence (RTP) materials. The abundant energy levels in PCDs increase the probability of intersystem crossing (ISC) and their covalently-crosslinked framework structures greatly suppress the non-radiative transitions. The efficient methods allow the manufacture of PCDs with unique RTP properties in air without the need for additional metal complexing or for the adopting of complicated matrix compositing. They thus provide a route towards the rational design of metal-free RTP materials that may be synthesized easily. Furthermore, we find that RTP is associated with crosslink enhanced emission (CEE) effect, which provides further routes to design improved PCDs with diverse RTP performance. Our results demonstrate the potential of PCDs as a universal route to achieve effective metal-free RTP.

Materials with long-lived excited states, affording special visualized performance with delayed luminescence^[1], are of great interest in applications such as photoelectricity^[2], photocatalysis^[3], imaging^[4], and security^[5]. Phosphorescence^[6], as one of the most interesting delayed-luminescence subtypes, has attracted extensive attention in recent years. However, due to the fact that phosphorescence is hampered by the spin-forbidden nature of triplet exciton transitions and by non-radiative decay processes, ultralow temperatures are often required to achieve effective phosphorescence. To overcome this, many approaches have been adopted to achieve room temperature phosphorescence (RTP). They follow two principles: one focuses on enhancing spin-orbit coupling by the introduction of transition metals, halogens, aromatic carbonyl or heterocycle groups to promote intersystem crossing efficiency^[6b]; the other seeks to restrict vibration and rotation by crystallization-guidance, matrix-assistance, or supramolecular interactions to suppress non-radiative transitions^[7]. Abundant attempts have been reported in the search for RTP materials, which can be broadly divided into those based on the use of organometallic complexes (metal-containing) and those focusing on pure organic compounds (metal-free). The metal coordination-based

RTP materials^[6b, 8] (generally making use of iridium, platinum, and other noble metals) suffer both from high cost and toxicity, while metal-free RTP alternatives^[5a, 6b, 9] which are dominated by several special organic moieties, such as aromatic carbonyl, heavy halogen, and deuterated carbon, are limited in chemical diversity and the complexity of their synthesis. There is a pressing need for new metal-free RTP materials with long lifetimes which can be manufactured using inexpensive synthesis routes.

As an emerging class of luminescent nanomaterials, carbon dots^[10] (CDs) have attracted sustained attention due to their superior luminescence, low toxicity, great stability, and ease of manufacture. Exciting reports about the fluorescence of CDs in solution are promising, but the investigation on solid-state luminescence of CDs is less extensive. Recently, unique RTP phenomena have been reported for CDs composite forms in a two-step blending synthesis route. RTP properties have been sought by embedding CDs into a variety of matrices, including polyvinyl alcohol^[11], polyurethane^[11c, 12], potassium aluminum sulfate^[13], recrystallized urea/biuret^[14], and layered double hydroxides^[15], demonstrating the potential of intersystem crossing (ISC) in CDs and suggesting that CDs might be promising candidates for metal-free RTP materials. The two-stage strategy to achieve RTP via hydrogen bonds and physical immobilization in additional matrices, however, raises challenges. In particular the stability of reversible interactions in such composites is an issue and has, thus far, limited the practical applications of these materials as metal-free RTPs.

Polymer carbon dots^[6] (PCDs), however, with abundant highly-crosslinked structures of non-conjugated groups, offer an alternative, novel and promising approach to achieving the elusive metal-free RTP via an extremely convenient synthesis approach. PCDs inherit the advantages of both facets of composite-based CDs materials, possessing both the excellent luminescent properties of CDs as well as the matrix effects imbued by polymers, which can substitute covalent bonds for supramolecular interactions and thus greatly enhance the fixation.

Here, we report the results for a series of PCDs systems that we have investigated in a bid to design a route to the production of metal-free RTP materials that is green, facile and cost-effective. Our computational simulations indicate that the covalent crosslinking occurring in the interior of PCDs can generate luminescence centers while simultaneously restricting their vibration and rotation, thus providing favorable conditions for effective ISC. To verify the feasibility of these computational predictions, we designed a new model system using polyacid and diamine to synthesize PCDs via a one-step hydrothermal treatment. Significant RTP performance was successfully found for our synthesized PCDs, as predicted. Employing results from both our experiments and our theoretical calculations, crosslink enhanced emission^[17] (CEE) effect has been proposed and verified as the RTP mechanism for PCDs. This provides an essential guide and insight into our novel route for the precise

[*] S.Tao, Y. Geng, Y. Song, T.Feng, Prof. W. Xu and Prof. B. Yang
State Key Laboratory of Supramolecular Structure and Materials,
College of Chemistry, Jilin University, Changchun, 130012, P. R.
China.

E-mail: byangchem@jlu.edu.cn

Dr S. Lu

College of Chemistry and Molecular Engineering, Zhengzhou
University, 100 Kexue Road, Zhengzhou 450001 China.

Dr S. Zhu

Laboratory of Molecular Imaging and Nanomedicine, National Institute
of Biomedical Imaging and Bioengineering, National Institutes of
Health, 35 Convent Dr, Bethesda, MD 20892 USA.

Prof. S. A. T Redfern

University of Cambridge, Department of Earth Sciences Downing
Street Cambridge, UK CB2 3EQ.

[*] These authors contributed equally to this work.

Supporting information for this article is given via a link at the end of
the document.

COMMUNICATION

WILEY-VCH

synthesis of these functional materials. Following this principle, together with our understanding of the key nature of raw materials, a wide variety of PCDs with diverse RTP properties could be subsequently designed and obtained. Thus, this work provides an effective strategy to the design, synthesis and application of efficient metal-free RTP materials, demonstrating a clear luminescence mechanism, and expands the application of PCDs into RTP fields as well as enriching the variety of metal-free RTP materials that may be deployed in device applications.

The first step in developing novel PCDs suitable for RTP applications is to select an appropriate model system. We focus on non-conjugated small molecules and linear polymers in order to avoid any possible conjugated components. In view of their abundant reactive groups and simple chemical structures, combined with the possibility that they offer for an extensive series of exploratory experiments, polyacrylic acid (PAA) and ethylenediamine (EDA) were selected as the raw materials for production of PCDs by a one-step hydrothermal method (see the Supporting Information). Synthesis was followed by dialysis and freeze-drying to remove unreacted raw materials and obtain solid final material. The purified solid product is here denoted as "PCDs₁₋₁".

The morphologies of PCDs₁₋₁ were characterized by transmission electron microscopy (TEM) and atomic force microscopy (AFM) to verify the generation of nanoparticles. The TEM image of PCDs₁₋₁ (Figure S1) displays well-dispersed nanodots with an average diameter of approximately 5.4 nm. No obvious lattice fringes can be observed in most dots, demonstrating the preservation of polymeric structures and avoidance of high-temperature carbonization. The AFM image reveals their topographic heights are homogeneously distributed in the range of 4 to 6 nm (Figure S2), consistent with the TEM results and previous reports^[18], indicating high morphological uniformity for our PCDs₁₋₁. X-ray diffraction (XRD) pattern displays two broad peaks at 21.2° and 38.9° (Figure S3), assigned to partial order in the interior of PCDs₁₋₁ resulting from covalently-crosslinked frameworks^[16a].

In the search for new bright-luminescent fluorophore materials, we focused on the investigation of fluorescence and phosphorescence in our samples. The colorless and transparent solution of PCDs₁₋₁ that we produced exhibits strong blue fluorescence but no phosphorescence. Its photoluminescence (PL) spectra show characteristic excitation-dependent fluorescence with optimal emission centered at around 410 nm (Figure 1a). Interestingly, the yellowish PCDs₁₋₁ powder exhibits blue emission under UV irradiation and blue-green afterglow once UV illumination is turned off (Supporting Movie). The alternating process has been caught by time resolved PL spectra (Figure S4). The PL spectra of PCDs₁₋₁ powder display similar excitation-dependent property to those of their solution, while the presence of phosphorescence may be responsible for the widened peaks and the long tail to higher wavelength (Figure 1b). The afterglow spectrum (Figure 1c) records the phosphorescence emission behavior of PCDs₁₋₁, with a broad peak from 425 nm to 700 nm, mainly centered at around 494 nm. Thus, benefiting from inherent polymeric structure, PCDs₁₋₁ successfully overcome the aggregation-caused quenching problem that afflicts most solid CDs, and at the same time possess excellent solid-state fluorescence and unique RTP properties without the need for additional matrix or composite structure.

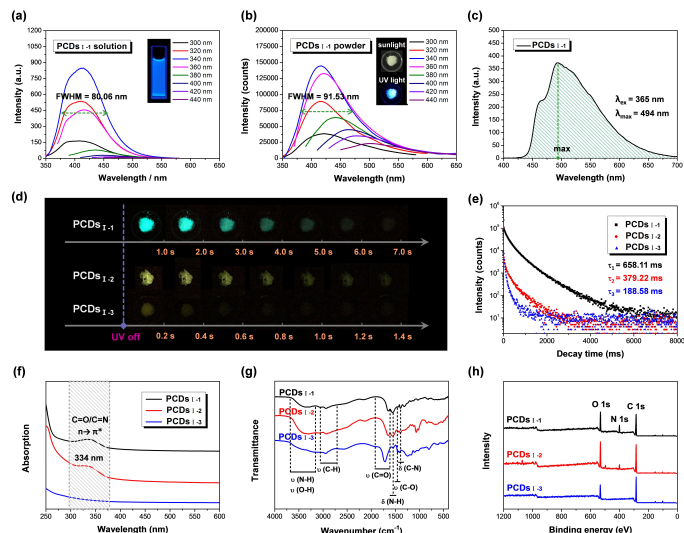


Figure 1 Property characterizations of PCDs. (a) Excitation dependence PL spectra of PCDs₁₋₁ aqueous solution (inset: photograph of aqueous solution under UV light). (b) Excitation-dependent PL spectra of PCDs₁₋₁ powder (inset: photographs of powder under sunlight or UV light). (c) Afterglow spectra of PCDs₁₋₁ powder. Comparative analysis of PCDs₁₋₁, PCDs₁₋₂, and PCDs₁₋₃: (d) Corresponding photographs at different delay time after UV irradiation. (e) RTP decay spectra. (f) UV-vis absorption spectra. (g) FTIR spectra. (h) XPS survey spectra.

Conjugated aromatic carbonyl compounds, sometimes with specific substituent groups, are widely recognized as the typical origin of phosphorescence in RTP materials. However, as seen from the ¹H NMR spectrum (Figure S5), the absence of characteristic chemical shifts in the aromatic region indicates the special nature of the RTP origin in PCDs₁₋₁, which appears unrelated to aromatic carbonyl. Based on the extensive study on fluorescence of CDs, it is generally accepted that the presence of nitrogen raises Fermi level and increases PL quantum yield (QY) by enriching electron and decreasing surface defects. In view of this, it is reasonable to suppose that nitrogen-related groups may be the cause of RTP in PCDs₁₋₁. To test the hypothesis, a set of contrast experiments was designed by replacing EDA with ethanolamine or ethylene glycol to prepare PCDs with similar structures but different nitrogen contents. The elemental analysis results of our substituted PCDs, named as PCDs₁₋₂ and PCDs₁₋₃ respectively, are shown in Table S1.

The images in Figure 1d illustrate the huge difference in RTP performance among these three samples. PCDs₁₋₁ exhibit the strongest emission and the longest delay (658.11 ms), followed by PCDs₁₋₂ (379.22 ms), while PCDs₁₋₃ show almost no RTP effect (Figure 1e, Table S2). After illumination by 365 nm UV radiation, the RTP signals of PCDs₁₋₁ and PCDs₁₋₂ can be observed as distinct emission bands, but any RTP from PCDs₁₋₃ approaches the level of the noise (Figure S6). The QYs of PCDs₁₋₁, PCDs₁₋₂ and PCDs₁₋₃ (Table S3) are measured to be 32.41%, 12.29%, 2.61% in aqueous solution and 28.77%, 11.17%, 2.13% in solid state, demonstrating the great contribution of nitrogen to luminescence (for both fluorescence and phosphorescence). UV-visible (UV-vis) absorption spectra (Figure 1f) reveal the n→π* transition of C=O/C=N bonds at about 334 nm. Notably, the presence of C=O or C=N groups has previously been reported to facilitate the generation of intrinsic triplet excitons through ISC^{30,34}. Fourier transform infrared (FTIR) spectra (Figure 1g) show the similar absorption curves of PCDs₁₋₁ and PCDs₁₋₂, which are obviously distinct from PCDs₁₋₃.

COMMUNICATION

WILEY-VCH

The characteristic vibrations for N-H (3349 and 1554 cm^{-1}), C=O/C=N (1647 cm^{-1}), and C-N (1309 cm^{-1}), indicate the presence of amide bonds. X-ray photoelectron spectroscopy (XPS) spectra (Figure 1h) display three typical peaks of C (285 eV), N (400 eV) and O (532 eV) in PCDs_{I-1} and PCDs_{I-2}, while only C (285 eV) and O (532 eV) in PCDs_{I-3}.

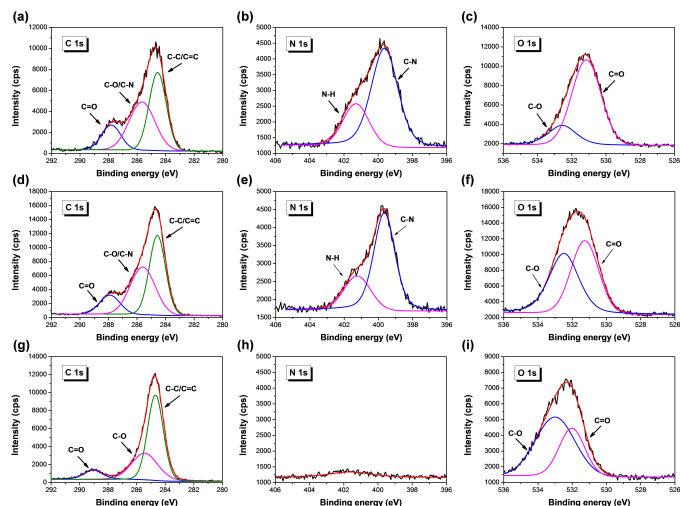


Figure 2 XPS characterization for bonding styles inside PCDs. (a) C 1s spectra, (b) N 1s spectra, and (c) O 1s spectra of PCDs_{I-1}. (d) C 1s spectra, (e) N 1s spectra, and (f) O 1s spectra of PCDs_{I-2}. (g) C 1s spectra, (h) N 1s spectra, and (i) O 1s spectra of PCDs_{I-3}.

The high-resolution XPS results (Figure 2) reveal the differences in the surface of the three samples. For PCDs_{I-1} and PCDs_{I-2}, the C 1s bands are deconvoluted into three similar peaks at 284.7 eV, 285.6 eV and 287.8 eV corresponding to C-C/C=C, C-O/C-N and C=O respectively. The N 1s analysis reveals the presence of C-N (399.6 eV) and N-H (401.3 eV). The O 1s band contains two peaks at 531.2 and 532.6 eV for C=O and C-O, respectively. The analysis above demonstrates the similar bonding styles of PCDs_{I-1} and PCDs_{I-2}, obviously distinct from that of PCDs_{I-3}. However, the major difference between PCDs_{I-1} and PCDs_{I-2} is that PCDs_{I-1} display a stronger XPS signal at N 1s band and higher relative content of C=O, indicating that the structure with N-related C=O may play an important role in RTP emission.

The aqueous solutions of PCDs only emit fluorescence without phosphorescence (Figure S7) due to the violent collision caused by free movement of molecules. The analogous PL decay curves of PCDs_{I-1} and PCDs_{I-2} solutions (Figure S8) fit the lifetimes with two similar exponential components (Table S4), indicating their homologous luminescence origins as speculated above. Nevertheless, the great disparity of RTP performance in our solid-state materials demonstrates the different confinement abilities of PCDs_{I-1} and PCDs_{I-2} in harvesting triplet excited states. Clearly, the internal mechanism of RTP generation needs further consideration.

To confirm the hypothesis that structural characteristics of PCDs materials control their RTP properties, PAA and a variety of EDA analogues (ethanolamine, ethylene glycol, n-propylamine, n-methylethylenediamine, n-ethylethylenediamine, N,N-dimethylethylenediamine, N,N'-dimethylethylenediamine, 1,3-diaminopropane, and 1,4-diaminobutane) were selected to carry out the second set of contrast experiments. Identical synthesis conditions were adopted to those used previously to ensure effective comparison (see the Supporting Information).

Table 1 sets out the chemical names and structural formulas in detail, and the corresponding products are denoted as PCDs_{II-1} to PCDs_{II-7} in turn. It is immediately apparent that none of PCDs in the second series exhibit obvious RTP besides PCDs_{II-6} and PCDs_{II-7} (Table 1). For PCDs_{II-1}, n-propylamine is a type of monoamine, which can't serve as an effective crosslinker to connect adjacent polymer chains. For PCDs_{II-2}, PCDs_{II-3}, PCDs_{II-4}, and PCDs_{II-5}, the presence of substituents brings about large steric hindrance for crosslinking reactions, disordering the crosslinked frameworks. Hence, no RTP phenomena are observed from PCDs_{II-1} to PCDs_{II-5} due to hindered crosslinking. But for PCDs_{II-6} and PCDs_{II-7}, the RTP of different intensities can be observed. The homologues of EDA, 1,3-diaminopropane and 1,4-diaminobutane possess extremely analogous chemical structures, and this eventually results in the similarity in the properties of their products. Compared with 1,3-diaminopropane, the longer alkyl chain in 1,4-diaminobutane allows greater freedom of vibration and rotation, decreasing the confinement ability of the crosslinked frameworks, and this thus weakens the RTP performance. Interestingly, all of the samples in the second series (Table 1) emit phosphorescence at ultralow temperature (77 K, in liquid nitrogen) since the nonradiative transitions at such temperature are largely suppressed. This indicates that the potential luminescence centers are present in all these materials, which is consistent with our explanation for the origin of phosphorescence. Taken together, all our data indicate that amide and/or imide emission centers exist in all the investigated PCDs, but phosphorescence only arises when efficient crosslinking exists.

	Chemical Name	Structural Formula	Room Temperature	77 K
I-1	ethylenediamine	<chem>NCCN</chem>	√	√
I-2	ethanolamine	<chem>NCCO</chem>	weak	√
I-3	ethylene glycol	<chem>OCCO</chem>	×	×
II-1	n-propylamine	<chem>NCCC</chem>	×	√
II-2	n-methylethylenediamine	<chem>CNCCN</chem>	×	√
II-3	n-ethylethylenediamine	<chem>CCNCCN</chem>	×	√
II-4	N,N-dimethylethylenediamine	<chem>CN(C)CCN(C)C</chem>	×	√
II-5	N,N'-dimethylethylenediamine	<chem>CN(C)CCN(C)C</chem>	×	√
II-6	1,3-diaminopropane	<chem>NCCCN</chem>	√	√
II-7	1,4-diaminobutane	<chem>NCCCCN</chem>	weak	√

√: Obvious RTP phenomenon can be observed after UV irradiation. Weak: Unobvious RTP phenomenon can be observed after UV irradiation. ×: No RTP phenomenon can be observed after UV irradiation. □: No luminescence center. ■: Hindered crosslinked frameworks.

Table 1 Summarized phosphorescence properties of PCDs powders at room temperature or 77 K synthesized by PAA and other EDA analogues: PCDs_{I-1}, PCDs_{I-2}, and PCDs_{I-3} (for luminescence origins), PCDs_{II-1}, PCDs_{II-2}, PCDs_{II-3}, PCDs_{II-4}, PCDs_{II-5}, PCDs_{II-6}, and PCDs_{II-7} (for crosslinking effect).

For scientific verification, we proposed several bonding configurations inside our PCDs (Figure 3a) according to the above results (XPS, NMR, comparative experiments). Based on the simplified structural units (Figure S9), theoretical calculations were further carried out to gain deeper insights into the mechanism of phosphorescence. Initially, we optimized the ground and triplet states of the unit cell (single luminescence unit, Figure 3b), and dimmer (coupled luminescence units, Figure 3c), and then we calculated the maximum

COMMUNICATION

WILEY-VCH

phosphorescence wavelength and lifetime. Our results suggest that the dimmer restricted unit (Figure 3c) has a maximum phosphorescence wavelength at 494 nm which agrees well with the experimental measurement. The ISC process mainly occurs from the HOMO to LUMO which involves the $n \rightarrow \pi^*$ transition between two repeated units polyacides ($N(C=O)_2$) linked through CH_2-CH_2 . Besides, a reasonable long lifetime of 0.03 s was also found, suggesting the contribution of coupled structure to potential phosphorescence in PCDs. In respect of the single luminescence unit, the maximum phosphorescence wavelength and lifetime were calculated to be 682 nm and 0.09 s, respectively, also involved to the $n \rightarrow \pi^*$ transition between the two polyacides ($N(C=O)_2$) as dimmer. However, the corresponding experiment didn't observe phosphorescence. The main reason could be the fact that in the real photoexcitation process, the CH_2-CH_2 should be able to rotate, that blocks the transition process of ISC and consequently quenches the phosphorescence. This is supported by the barrier less rotation profile for the single unit (Figure S10). Thus, crosslinking and polymerizing are beneficial to fix and restrict the rotation motion of CH_2-CH_2 . Meanwhile, we found large difference exists in the bond length of C=O and N-C as given in Figure S11. For single unit, C=O and N-C show more double bond character, while for dimmer, in particular for T_1 , the C=O has less double bond character. Therefore, the dimmer has poor π -electron conjugation as compared to single unit. This also brings about narrowed ΔE_{ST} in favor of ISC. Fortunately, the structure of PCDs provides favorable conditions for the generation of triplet excitons, bringing about the unique RTP performance.

In our earlier studies, we confirmed the important role of crosslinking in non-conjugated PCDs that only possess subfluorophores (such as C=O, C=N, N=O), and proposed the crosslink enhanced emission^[16a, 16c, 17] (CEE) effect as the origin of enhanced PL. Here, CEE effect is also deemed to be responsible for the generation of RTP in PCDs, which could provide a basis to design materials with such properties. This approach is successfully verified as judged by the phosphorescent behavior of our PCDs measured at both room temperature and ultralow temperature (Table 1).

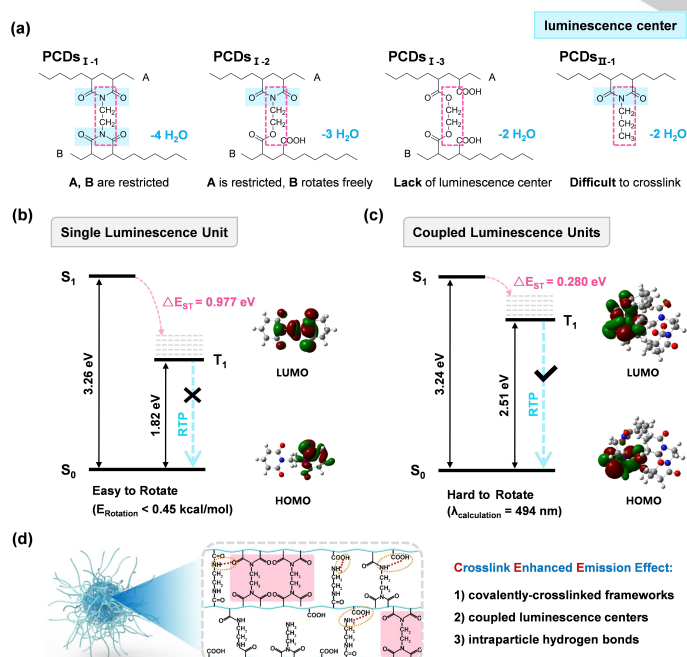


Figure 3 Summarized formation process of RTP performance in PCDs. (a) Schematic structure of crosslinking sites. PCDs₁₋₁: EDA, PCDs₁₋₂: ethanolamine, PCDs₁₋₃: ethylene glycol, and PCDs_{II-1}: n-propylamine. Theoretical analysis of CEE effect: (b) Energy level diagrams of single luminescence unit and (c) coupled luminescence units. (d) Schematic illustration of CEE effect.

If we consider PCDs₁₋₁ as an example, the contribution of CEE effect to RTP is mainly reflected in three aspects (Figure 3d): Firstly, chemical reactions take place easily among the abundant functional groups. EDA can serve as a crosslinker to react with extensive dangling carboxyl groups on polymer chains and further form covalently-crosslinked frameworks. The self-matrix structures can effectively suppress the non-radiative transitions by covalently bonding emissive centers and interrupting the motion of polymer chains. Secondly, the entanglement and crosslinking in high degree greatly restricts the intraparticle space of PCDs and simultaneously shortens the distance between functional groups. New distributions of energy levels can be formed by electron overlap from coupled luminescence units in the nano-confined space, and this can effectively reduce the energy gap (ΔE_{ST}) and facilitate the generation of intrinsic triplet. Thirdly, in addition to any specific immobilization associated with covalent bonding, PCDs materials also possess complex intraparticle hydrogen bonds, distinguished from the interaction between emissive species and additional matrices of commonly-reported RTP materials. The widespread existence of supramolecular interactions in the interior of PCDs can further decrease vibration and rotation, thus inhibiting any non-radiative relaxation. Hence, covalently-crosslinked frameworks, coupled luminescence centers, and intraparticle hydrogen bonds caused by CEE effect contribute to the generation of RTP in PCDs together.

Further work was carried out to explore the effects of different synthesis methods via PAA and EDA, including refluxing (PCDs_{III-1}), EDC/NHS crosslinking (PCDs_{III-2}) and physically compositing (PCDs_{III-3}) (see the Supporting Information). The results show phosphorescent properties of PCDs₁₋₁ are doubtlessly superior to all the manufactured PCDs in the third series (Table S5). This is because the extremely high temperature and pressure conditions of hydrothermal process increases the collision, entanglement and crosslinking among polymer chains, ultimately endowing PCDs with denser and better-crosslinked internal structure. It is confirmed again that CEE effect plays an important role in arriving at PCDs with good RTP performance.

To our delight, our PCDs₁₋₁ have a pretty high production yield up to 63.1% (Table S6) and good stability after UV exposure (Figure S12). Moreover, PCDs₁₋₁ still exhibit RTP performance even after being ground into a fine powder (Supporting Movie), indicating the strong resistance endowed by covalently crosslinking to external damage.

By adopting PCDs₁₋₁, PCDs₁₋₂, commercial highlighters and reported CDs^[10b], graphic security and information encryption have been respectively designed to provide a simple demonstration of the promising applications of PCDs as a smart material in security protection. As shown in Figure 4, a colorful butterfly and "Just Love U" are visible under 365 nm UV illumination. Once the excitation is switched off, a changed butterfly pattern and "JLU" are seen as a result of the intrinsic emission differences between PL and RTP, and distinctive RTP performance of different PCDs materials.

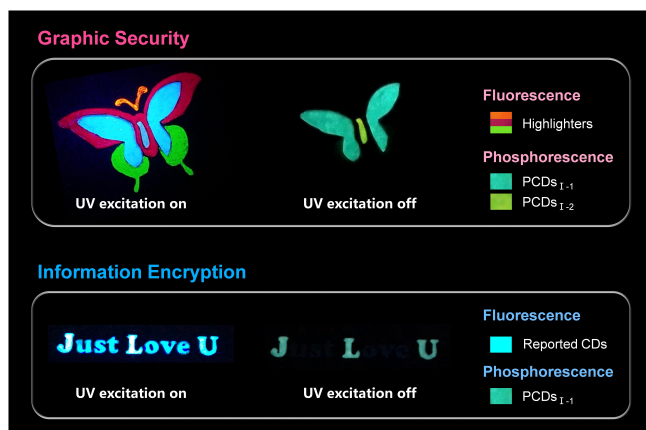


Figure 4 Photographs of graphic security and information encryption made from PCDs₁₋₁, PCDs₁₋₂, commercial highlighters and reported CDs.

In summary, we describe a feasible and facile route to produce metal-free RTP materials by directly constructing PCDs via hydrothermal synthesis without the need for additional matrices compositing. As a model system, the PCDs materials synthesized from PAA and EDA show unique RTP properties in air as expected, demonstrating the utility of our approach. The PCDs structures with amide or imide, alongside the CEE effect were confirmed to both contribute to the generation of RTP in PCDs. Given the wide range of chemical precursors and possible synthesis conditions, we suggest that our approach can lead to a wide variety of PCDs materials with diverse engineered RTP properties. Careful selection of precursors, such as combinations of polyacid, polyamine, polyolol, diacid, diamine or other potential multifunctional compounds, and different synthesis routes, such as solvothermal or even ultrasonic/microwave assisted hydrothermal/solvothermal treatment, provide a wide range of potential routes to the formation of PCDs materials tuned to specific applications. Our findings shine a new light on the problem of generating metal-free RTP materials. We show significant RTP performance with PCDs, and propose the adoption of PCDs in delayed luminescence-related applications. Additionally, this class of materials opens the way to the design of a new class of metal-free RTP materials. We also anticipate the emergence of novel biosystems that will further expand the RTP properties for specific biomaterials.

Acknowledgements

This work was financially supported by the National Science Foundation of China (NSFC) under Grant Nos. 51433003, 51373065, 21504029, the National key research and development program of China (2016YFB0401701) and JLU Science and Technology Innovative Research Team 2017TD-06.

Keywords: luminescent materials • polymer carbon dots • metal-free • room temperature phosphorescence • crosslink enhanced emission effect

[1] a) J. Liu, N. Wang, Y. Yu, Y. Yan, H. Zhang, J. Li, J. Yu, *Science advances* **2017**, *3*, e1603171-e1603171; b) Q. Zhang, B. Li, S. Huang, H. Nomura, H. Tanaka, C. Adachi, *Nature Photonics* **2014**, *8*, 326-332; c) H. Uoyama, K. Goushi, K. Shizu, H. Nomura, C. Adachi, *Nature* **2012**, *492*, 234-+.

[2] a) H. Xu, R. Chen, Q. Sun, W. Lai, Q. Su, W. Huang, X. Liu, *Chemical Society Reviews* **2014**, *43*, 3259-3302; b) L. Xiao, Z. Chen, B. Qu, J. Luo, S. Kong, Q. Gong, J. Kido, *Advanced Materials* **2011**, *23*, 926-952.

[3] J. Zhao, W. Wu, J. Sun, S. Guo, *Chemical Society Reviews* **2013**, *42*, 5323-5351.

[4] a) G. Zhang, G. M. Palmer, M. Dewhurst, C. L. Fraser, *Nature Materials* **2009**, *8*, 747-751; b) S. Cai, H. Shi, J. Li, L. Gu, Y. Ni, Z. Cheng, S. Wang, W.-w. Xiong, L. Li, Z. An, W. Huang, *Advanced Materials* **2017**, *29*, n/a-n/a.

[5] a) Z. An, C. Zheng, Y. Tao, R. Chen, H. Shi, T. Chen, Z. Wang, H. Li, R. Deng, X. Liu, W. Huang, *Nature Materials* **2015**, *14*, 685-690; b) H. Sun, S. Liu, W. Lin, K. Y. Zhang, W. Lv, X. Huang, F. Huo, H. Yang, G. Jenkins, Q. Zhao, W. Huang, **2014**, *5*, 3601.

[6] a) Z. He, W. Zhao, J. W. Y. Lam, Q. Peng, H. Ma, G. Liang, Z. Shuai, B. Z. Tang, *Nature Communications* **2017**, *8*; b) J. Mei, N. L. C. Leung, R. T. K. Kwok, J. W. Y. Lam, B. Z. Tang, *Chemical Reviews* **2015**, *115*, 11718-11940.

[7] a) D. Lee, O. Bolton, B. C. Kim, J. H. Youk, S. Takayama, J. Kim, *Journal of the American Chemical Society* **2013**, *135*, 6325-6329; b) M. S. Kwon, D. Lee, S. Seo, J. Jung, J. Kim, *Angewandte Chemie International Edition* **2014**, *53*, 11177-11181; c) H. A. Al-Attar, A. P. Monkman, *Advanced Functional Materials* **2012**, *22*, 3824-3832; d) Y. Gong, Y. Tan, H. Li, Y. Zhang, W. Yuan, Y. Zhang, J. Sun, B. Z. Tang, *Science China Chemistry* **2013**, *56*, 1183-1186.

[8] a) S. Lamansky, P. Djurovich, D. Murphy, F. Abdel-Razzaq, H. E. Lee, C. Adachi, P. E. Burrows, S. R. Forrest, M. E. Thompson, *Journal of the American Chemical Society* **2001**, *123*, 4304-4312; b) Y. Chi, P.-T. Chou, *Chemical Society Reviews* **2010**, *39*, 638-655; c) Q. Zhao, F. Li, C. Huang, *Chemical Society Reviews* **2010**, *39*, 3007-3030.

[9] a) O. Bolton, K. Lee, H.-J. Kim, K. Y. Lin, J. Kim, *Nat Chem* **2011**, *3*, 205-210; b) S. Hirata, K. Totani, J. Zhang, T. Yamashita, H. Kajji, S. R. Marder, T. Watanabe, C. Adachi, *Advanced Functional Materials* **2013**, *23*, 3386-3397.

[10] a) X. Y. Xu, R. Ray, Y. L. Gu, H. J. Ploehn, L. Gearheart, K. Raker, W. A. Scrivens, in *Journal of the American Chemical Society*, Vol. 126, **2004**, pp. 12736-12737; b) S. Zhu, Q. Meng, L. Wang, J. Zhang, Y. Song, H. Jin, K. Zhang, H. Sun, H. Wang, B. Yang, *Angewandte Chemie-International Edition* **2013**, *52*, 3953-3957; c) S. Lu, L. Sui, J. Liu, S. Zhu, A. Chen, M. Jin, B. Yang, *Advanced Materials* **2017**, *29*; d) S. Lu, G. Xiao, L. Sui, T. Feng, X. Yong, S. Zhu, B. Li, Z. Liu, B. Zou, M. Jin, J. S. Tse, H. Yan, B. Yang, *Angewandte Chemie-International Edition* **2017**, *56*, 6187-6191; e) W. Li, Z. Zhang, B. Kong, S. Feng, J. Wang, L. Wang, J. Yang, F. Zhang, P. Wu, D. Zhao, *Angewandte Chemie International Edition* **2013**, *52*, 8151-8155; f) J. Tang, B. Kong, H. Wu, M. Xu, Y. Wang, Y. Wang, D. Zhao, G. Zheng, *Advanced Materials* **2013**, *25*, 6569-6574.

[11] a) Y. Deng, D. Zhao, X. Chen, F. Wang, H. Song, D. Shen, *Chemical Communications* **2013**, *49*, 5751-5753; b) K. Jiang, L. Zhang, J. Lu, C. Xu, C. Cai, H. Lin, *Angewandte Chemie-International Edition* **2016**, *55*, 7231-7235; c) J. Tan, J. Zhang, W. Li, L. Q. Zhang, D. M. Yue, *Journal of Materials Chemistry C* **2016**, *4*, 10146-10153.

[12] J. Tan, R. Zou, J. Zhang, W. Li, L. Zhang, D. Yue, *Nanoscale* **2016**, *8*, 4742-4747.

[13] X. Dong, L. Wei, Y. Su, Z. Li, H. Geng, C. Yang, Y. Zhang, *Journal of Materials Chemistry C* **2015**, *3*, 2798-2801.

[14] Q. Li, M. Zhou, Q. Yang, Q. Wu, J. Shi, A. Gong, M. Yang, *Chemistry of Materials* **2016**, *28*, 8221-8227.

[15] L. Q. Bai, N. Xue, X. R. Wang, W. Y. Shi, C. Lu, *Nanoscale* **2017**, *9*, 6658-6664.

[16] a) S. Tao, S. Zhu, T. Feng, C. Xia, Y. Song, B. Yang, *Materials Today Chemistry* **2017**, *6*, 13-25; b) Y. Song, S. Zhu, J. Shao, B. Yang, *Journal of Polymer Science Part a-Polymer Chemistry* **2017**, *55*, 610-615; c) S. Y. Tao, Y. B. Song, S. J. Zhu, J. R. Shao, B. Yang, *Polymer* **2017**, *116*, 472-478.

[17] a) S. J. Zhu, L. Wang, N. Zhou, X. H. Zhao, Y. B. Song, S. Maharjan, J. H.

Zhang, L. J. Lu, H. Y. Wang, B. Yang, *Chemical Communications* **2014**, 50, 13845-13848; b) S. J. Zhu, Y. B. Song, J. R. Shao, X. H. Zhao, B. Yang, *Angewandte Chemie-International Edition* **2015**, 54, 14626-14637; c) S. Zhu, Y. Song, X. Zhao, J. Shao, J. Zhang, B. Yang, *Nano Research* **2015**, 8, 355-381.

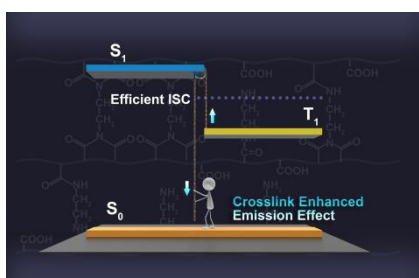
[18] a) D. Li, D. Han, S.-N. Qu, L. Liu, P.-T. Jing, D. Zhou, W.-Y. Ji, X.-Y. Wang, T.-F. Zhang, D.-Z. Shen, *Light-Science & Applications* **2016**, 5; b) M. Zheng, S. Liu, J. Li, D. Qu, H. Zhao, X. Guan, X. Hu, Z. Xie, X. Jing, Z. Sun, *Advanced Materials* **2014**, 26, 3554-3560.

WILEY-VCH

Accepted Manuscript

COMMUNICATION

We describe an efficient and facile method to achieve metal-free room temperature phosphorescence (RTP) by constructing polymer carbon dots (PCDs). We verify the contribution of crosslink enhanced emission effect to the generation of RTP, and propose it as a guideline to forecast and synthesize a series of PCDs with diverse RTP performance.



Songyuan Tao[†], Siyu Lu[†], Yijia Geng, Shoujun Zhu, Simon A. T Redfern, Yubin Song, Tanglue Feng, Weiqing Xu and Bai Yang^{*}

Page No. – Page No.

Design of Metal-Free Polymer Carbon Dots: a New Class of Room-Temperature Phosphorescent Materials

Accepted Manuscript